The Astrophysical Journal Letters, 851:L48 (6pp), 2017 December 20 https://doi.org/10.3847/2041-8213/aaa07d
© 2017. The American Astronomical Society. All rights reserved.

An Empirical Limit on the Kilonova Rate from the DLT40 One Day Cadence Supernova Survey

Sheng Yang[1,2], Stefano Valenti[1], Enrico Cappellaro[2], David J. Sand[3], Leonardo Tartaglia[1,3], Alessandra Corsi[4], Daniel E. Reichart[5], Joshua Haislip[5], and Vladimir Kouprianov[5]
[1] Department of Physics, University of California, 1 Shields Avenue, Davis, CA 95616-5270, USA
[2] INAF Osservatorio Astronomico di Padova, Vicolo dell'Osservatorio 5, I-35122 Padova, Italy
[3] Department of Astronomy/Steward Observatory, 933 North Cherry Avenue, Room N204, Tucson, AZ 85721-0065, USA
[4] Physics & Astronomy Department, Texas Tech University, Lubbock, TX 79409, USA
[5] Department of Physics and Astronomy, University of North Carolina at Chapel Hill, Chapel Hill, NC 27599, USA
Received 2017 October 15; revised 2017 December 6; accepted 2017 December 8; published 2017 December 21

Abstract

Binary neutron star mergers are important in understanding stellar evolution, the chemical enrichment of the universe via the *r*-process, the physics of short gamma-ray bursts, gravitational waves, and pulsars. The rates at which these coalescences happen is uncertain, but it can be constrained in different ways. One of those is to search for the optical transients produced at the moment of the merging, called a kilonova, in ongoing supernova (SN) searches. However, until now, only theoretical models for a kilonova light curve were available to estimate their rates. The recent kilonova discovery of AT 2017gfo/DLT17ck gives us the opportunity to constrain the rate of kilonovae using the light curve of a real event. We constrain the rate of binary neutron star mergers using the DLT40 Supernova search and the native AT 2017gfo/DLT17ck light curve obtained with the same telescope and software system. Excluding AT 2017gfo/DLT17ck due to visibility issues, which was only discovered thanks to the aLIGO/aVirgo trigger, no other similar transients were detected during the 13 months of daily cadence observations of ∼2200 nearby (<40 Mpc) galaxies. We find that the rate of BNS mergers is lower than 0.47–0.55 kilonovae per 100 years per $10^{10}\,L_{B_\odot}$ (depending on the adopted extinction distribution). In volume, this translates to $<0.99\times10^{-4+0.19}_{-0.15}$, $\mathrm{Mpc}^{-3}\,\mathrm{yr}^{-1}$(SNe Ia–like extinction distribution), consistent with previous BNS coalescence rates. Based on our rate limit, and the sensitivity of aLIGO/aVirgo during O2, it is very unlikely that kilonova events are lurking in old pointed galaxy SN search data sets.

Key words: stars: neutron – supernovae: general – surveys

1. Introduction

Binary neutron star (BNS) systems (Hulse & Taylor 1975) have been studied with great interest by the astronomical community because of their connection with many open problems of astrophysics, from short gamma-ray bursts (GRBs) to *r*-process element production and from the physics of very high density matter to gravitational waves. The number of known BNSs today is limited to a dozen systems (Lattimer 2012) and the rate of BNS coalescences is known with orders of magnitude of uncertainty (Abadie et al. 2010; Coward et al. 2012; Berger et al. 2013; Petrillo et al. 2013; Drout et al. 2014; Siellez et al. 2014; de Mink & Belczynski 2015; Dominik et al. 2015; Fong et al. 2015; Jin et al. 2015; Kim et al. 2015; Vangioni et al. 2016; Abbott et al. 2017a; Scolnic et al. 2017). The rate of BNS coalescences can be constrained from the population of galactic pulsars (Kalogera et al. 2004), from modeling the evolution of the binary system (de Mink & Belczynski 2015; Dominik et al. 2015), from the cosmic abundance of *r*-process elements (Vangioni et al. 2016), or from measuring the rate of short GRBs, most likely produced at the moment of the coalescence (Berger et al. 2013).

An alternative method to constrain the rate of BNS mergers is to constrain the rate of kilonovae detected in supernova (SN) search surveys. Kilonovae are thought to be the ubiquitous, isotropically emitting counterparts to neutron star mergers. They are expected to eject at very high velocity a small mass (0.01–0.05 M_{Sun}) mainly made of high opacity *r*-process heavy elements; hence, they are predicted to have a "red" spectrum, to be faint at maximum light ($M_V\sim-16$ mag), and to decline quickly over the course of 1–2 weeks (e.g., Metzger et al. 2010; Kasen et al. 2013; Piran et al. 2013). This is in contrast to the most common SNe, which evolve on 0–100 day timescales (e.g., see Figure 1.1 of Kasliwal et al. 2011).

One clear hindrance to calculating the kilonova rate has been the lack of observed kilonova events (with possible exceptions; see Jin et al. 2016 for a compilation) in ongoing transients searches. Some progress has been made by using theoretical kilonova light curves to calculate the upper limit of their rate in programs like the Dark Energy Survey (Doctor et al. 2017). Additionally, there have been several recent attempts to estimate the rate of fast optical transients that evolve on sub-day timescales ($\tau\sim0.5$ hr to 1 day; Berger et al. 2013) all the way up to ∼10 day timescales (Drout et al. 2014).

With the discovery of AT 2017gfo (Abbott et al. 2017a, 2017b), we can directly constrain the rate of kilonovae by using its light curve as a template while allowing for possible diversity in kilonova light curves and a range of extinction values. Here, we present the rate estimate for kilonovae using our observed light curve of AT 2017gfo and the data from the ongoing Distance Less Than 40 Mpc (DLT40) supernova search (Tartaglia et al. 2017). DLT40 is an SN search that points to galaxies within $D\lesssim40$ Mpc with a one day cadence.[6] Given the magnitude limit of the program ($r\sim19$ mag) DLT40 is well suited to detect a nearby kilonova event. An advantage of DLT40 is that we can directly use the light curve of AT 2017gfo obtained with the same instrumental setup

[6] See the next section for details on the DLT40 cadence.

(Valenti et al. 2017) to get a direct limit for similar transients in the DLT40 program.

This Letter is organized as follows. In Section 2, we describe the DLT40 search and the survey operation during the O2 run. In Section 3, we will highlight the steps necessary to measure the rates, while in Section 4 we will compare our results with previous rate estimates and discuss the future prospects on how the improve the rates with or independently from the next LIGO/Virgo observing run.

2. The DLT40 Search

DLT40 is a one day cadence[7] search for SNe, targeting galaxies in the nearby universe ($D \lesssim 40$ Mpc) and designed for the goal of discovering ~10 SNe per year within one day of explosion (Tartaglia et al. 2017). Running continuously since 2016 September, DLT40 observes ~400–600 galaxies every night using a 0.41 m PROMPT telescope (Reichart et al. 2005) at the Cerro Tololo Inter-American Observatory (CTIO).

With a field of view (FoV) of 10×10 arcmin^2, DLT40 is suitable for mapping nearby galaxies down to a limiting magnitude of $r \sim 19$ mag in 45 s unfiltered exposures. The DLT40 catalog includes galaxies from the Gravitational Wave Galaxy Catalog (GWGC; White et al. 2011) at a declination $<20°$, with an absolute magnitude $M_B < -18$ mag, galactic extinction $A_V < 0.5$ mag, and recessional velocity $v_r < 3000$ km s^{-1} (corresponding to $D \lesssim 40$ Mpc). An additional constraint is that the FoV should not include stars brighter than 8 mag. These selections led to a sample of 2220 bright galaxies. In Figure 1, we show the sky distribution of galaxies in the DLT40 catalog. By comparing the integrated luminosity of DLT40's galaxy sample with the total integrated luminosity of the GWGC catalog, we estimated that the DLT40 catalog contains ~60% of the total luminosity (and therefore roughly mass) of the GWGC catalog. Note that the GWGC is supposed to be complete out to 40 Mpc (White et al. 2011). The DLT40 galaxy catalog is not biased with respect to morphological type of galaxy (S. Yang et al. 2017, in preparation), but by construction it is biased against low-luminosity galaxies (for example, dwarf galaxies).

In order to find SNe within a day from explosion, the DLT40 data are processed in nearly real time. Pre-reduced images are transferred within ~1 minute to our dedicated server where new candidates are detected by image subtraction with respect to a template image (using `Hotpants`; Becker 2015) so that new candidates are available for scanning by human operator within a few minutes after acquisition. Confirmation images of new SN candidates are taken within a few hours of their DLT40 discovery, often with the Las Cumbres Observatory telescope network (Brown et al. 2013).

Since the beginning of the search (2016 September), we have discovered 26 SNe, 12 of which were first announced by DLT40. Seven were discovered within 48 h of explosion (see Table 1 for a list of transients discovered by DLT40). The late discovery of the remaining transients by DLT40 was due to poor weather conditions.

While searching for SNe, DLT40 also reacted to LIGO/Virgo triggers during the O2 observing run, prioritizing the galaxies from the DLT40 catalog within the LIGO/Virgo localization region for each trigger. Following the LIGO/Virgo trigger of GW170817 (LIGO Scientific Collaboration & Virgo Collaboration 2017a, 2017b), DLT40 independently discovered and monitored the evolution of the kilonova AT 2017gfo/DLT17ck (Valenti et al. 2017). Given the daily cadence of the search, DLT40 is well suited to discover similar fast kilonova-like transients. In the particular case of DLT17ck, we had to revise our target priority list because the GW localization placed it near the horizon at sunset in Chile. During the course of the normal survey, however, any other kilonova-like transient would have been visible in the DLT40 search fields, given that DLT17ck itself was ~1.5 mag brighter than our typical detection limit, out to the border of our $D \sim 40$ Mpc pointed search.

3. Rate Measurement

One approach to measuring the rate of an astronomical transient makes use of the *control time* concept (Zwicky 1942; Cappellaro et al. 1993, 1997). For each ith galaxy, the control time (ct_i) is defined as the time during which a hypothetical transient is above the detection limit. It depends on the magnitude limit of each observation and the light curve of the transient. The total control time per unit luminosity of our search is computed by multiplying the ct_i control time by the luminosity of the ith galaxy and then summing over all of the galaxies in our sample[8]:

$$ct = \sum_{i=1}^{n} L_i^* ct_i.$$

The ratio between the number of transients detected and the sum of the control times for all galaxies observed gives immediately the rate as

$$r = \frac{N}{ct}.$$

In order to measure the control time, the first step is evaluate the transient detection efficiency for each image or, in other words, to measure the apparent magnitude limit for transient detection. In order to do that, we performed artificial star experiments for a subset of frames, implanting stars with different magnitudes using the proper point-spread functions (PSFs) and registering the fraction of artificial stars automatically identified by our pipeline on the difference images.

Hereafter, we will adopt the magnitude corresponding to a 50% detection efficiency as the limiting magnitude for the DLT40 survey, while we use the 16% and 84% detection efficiencies as lower/upper limits to determine its uncertainty. We found that the magnitude limit of our search is in the range $M_r \sim 18$–20 mag (see the left panel of Figure 2) depending on weather and seeing conditions of the specific observation. Since artificial star experiments are time consuming, instead of repeating the simulation for all of the ~120,000 frames observed so far, we exploited a linear relation between the limiting magnitude for transient detection computed through artificial star experiments and the limiting magnitude for stellar source detection computed for each target frame (i.e., not the difference image). The latter was derived through an analytic equation using information on the noise and photometric calibration for each image. The comparisons between the two

[7] This is the goal; however, the reader should be aware that weather losses and technical problems may randomly affect our cadence of observations. For example, during the first year of DLT40 14% nights were lost because of weather or technical problems.

[8] The control time ct_i depends also on the absolute magnitude of the transient (brighter transients will remain visible for a longer time above threshold).

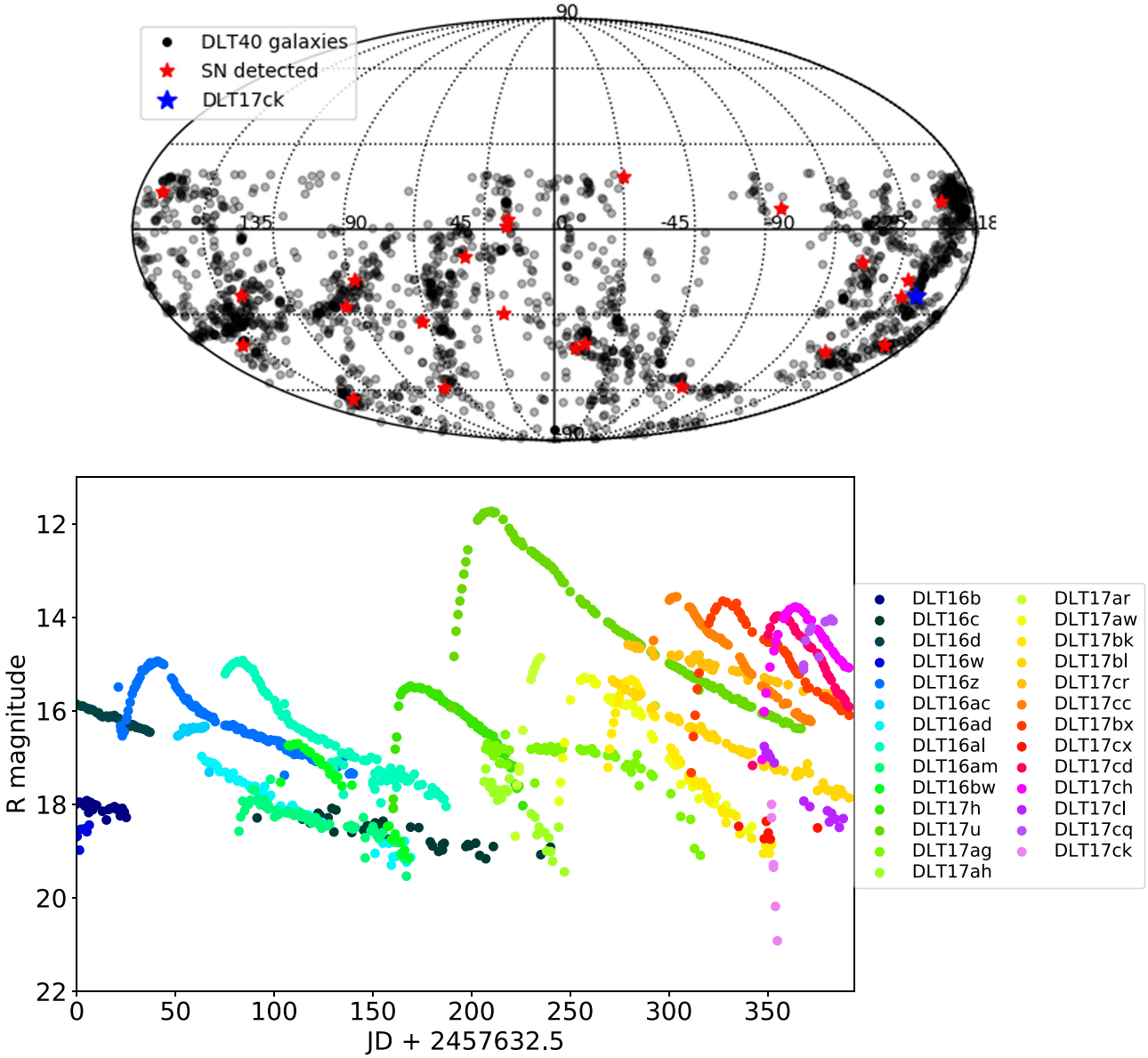

Figure 1. Top panel: the DLT40 galaxy catalog (black points). The SNe discovered during the first year of DLT40 are also shown (red points) together with the kilonova DLT17ck (blue point). Lower panel: DLT40 light curves of all of the SNe (and the kilonova) discovered during the first year of the search.

limiting magnitudes is shown in the right panel of Figure 2. In general, the limiting magnitude computed with the analytic function on the target image (y axes) is $\sim$1 mag deeper than the limit magnitude from artificial stars experiment (x axes). This is expected since the difference imaging technique effectively adds the template image noise to that of the target image.

The second ingredient to measure the control time is the simulation of kilonova light curves in the time window each galaxy was observed. The time that the transient is above our detection limit contributes to the control time. The observed light curve of AT 2017gfo/DLT17ck was used as a reference, scaled to the distance of each galaxy with an explosion epoch randomly distributed in the observed time window. We took into account that kilonovae may have a range of absolute magnitudes and that they may experience a variety of host galaxy extinction due to dust. For the range in kilonova magnitudes, we varied the absolute magnitude of the kilonova using a Gaussian distribution centered on the absolute magnitude of AT 2017gfo/DLT17ck and a σ of 0.5 mag (e.g., 95% of simulated light curves have an absolute magnitude within $\pm$1 mag of AT 2017gfo/DLT17ck). For the extinction distribution, we notice that the host environment of neutron stars mergers is often compared to the host environment of SNe Ia since both types of systems are found in early-type and star-forming galaxies (Fong et al. 2013). For this reason, we adopted for the extinction distribution $P(A_V) = e^{-A_V/\tau_V}$, with $\tau_V = 0.334 \pm 0.088$ mag (Kessler et al. 2009), which we label the "SN Ia extinction" scenario. We also computed the control time using either no extinction (low extinction scenario) or an extinction distribution with a τ value inflated by a factor of 2 (high extinction scenario). We want to stress that, given that DLT17ck is the first clear case of a kilonova, any choice of absolute magnitude range and reddening law is somehow arbitrary and those quantities will be better constrained when a larger number of kilonovae are discovered.

In summary, for each galaxy, we have simulated 20,000 light curves randomly distributed in the 13 months of the search, with a range of absolute magnitudes and reddening. If at any epoch of observation the simulated light curve was brighter

Table 1
Summary Table of the Supernovae Detected with DLT40

R.A.	Decl.	DLT Name	TNS Name	SN Type	Host Galaxy
278.63	−58.53	DLT16b	2016bmi	SN IIp	IC4721
170.08	12.98	DLT16c	2016cok	SN IIp	NGC3627
329.77	18.19	DLT16d	2016coi	SN Ic	UGC11868
328.62	−57.66	DLT16w	2016fjp	SN Ia	BKG
23.56	−29.44	DLT16z	2016gkg	SN IIb	NGC0613
20.55	0.95	DLT16ac	2016hgm	SN II	NGC0493
140.87	−23.17	DLT16ad	2016gwl	SN Ia	NGC2865
63.02	−32.86	DLT16al	2016iae	SN Ic	NGC1532
63.03	−32.85	DLT16am	2016ija	SN II	NGC1532
114.29	−52.32	DLT16bw	2016iyd	SN II	BKG
159.32	−41.62	DLT17h	2017ahn	SN II	NGC3318
218.14	−44.13	DLT17u	2017cbv	SN Ia	NGC5643
193.46	9.70	DLT17ag	2017cjb	SN II	NGC4779
200.52	−13.14	DLT17ah	2017ckg	SN II	BKG
144.15	−63.95	DLT17ar	2017cyy	SN Ia	ESO091-015
263.11	7.06	DLT17aw	2017drh	SN Ia	NGC6384
192.15	−41.32	DLT17bk	2017ejb	SN Ia	NGC4696
349.06	−42.57	DLT17bl	2017bzc	SN Ia	NGC7552
344.32	−41.02	DLT17cr	2017bzb	SN II	NGC7424
227.31	−11.33	DLT17cc	2017erp	SN Ia	NGC5861
20.06	3.40	DLT17bx	2017fgc	SN Ia	NGC0474
114.11	−69.55	DLT17cx	2016jbu	SN IIn	NGC2442
95.39	−27.21	DLT17cd	2017fzw	SN Ia	NGC2217
71.46	−59.25	DLT17ch	2017gax	SN Ibc	NGC1672
88.27	−17.87	DLT17cl	2017gbb	SN Ia	IC0438
38.88	−9.35	DLT17cq	2017gmr	SN II	NGC0988
197.45	−23.38	DLT17ck	2017gfo	kilonova	NGC4993

Note. Their light curves are shown in Figure 1. Supernovae detected in background galaxies are marked as BKG.

Table 2
DLT40 Rate Estimation Results

Type	Extinction (mag)	Control Time (days)	Lums Rate[a] (SNuB)	Vol Rate[b] (10^{-4} Mpc^{-3} yr^{-1})	Milky Way Rate[c] ((100 yr)$^{-1}$)
No Reddening	$P(A_V) = 0$	$79.67^{+4.51}_{-5.53}$	$<0.47^{+0.04}_{-0.03}$	$<0.93^{+0.16}_{-0.18}$	$<0.94^{+0.38}_{-0.37}$
Ia Reddening	$P(A_V) = e^{-A_V/0.334}$	$75.07^{+5.35}_{-6.56}$	$<0.50^{+0.05}_{-0.04}$	$<0.99^{+0.19}_{-0.15}$	$<1.00^{+0.43}_{-0.36}$
High Reddening	$P(A_V) = 2 \times e^{-A_V/0.334}$	$69.46^{+6.15}_{-7.28}$	$<0.55^{+0.07}_{-0.05}$	$<1.09^{+0.24}_{-0.18}$	$<1.10^{+0.51}_{-0.40}$

Notes.
[a] DLT40 only detected DLT17ck because of the LIGO detection and subsequent localization; therefore, it is not considered in our rate calculations, which we report here as 95% confidence level Poisson single-sided upper limits, given zero events (Gehrels 1986).
[b] We converted the rates in units of SNuB to volumetric rates with luminosity density: $(1.98 \pm 0.16) \times 10^{-2} \times 10^{10}\, L_{\odot}^{B}$ Mpc^3 (Kopparapu et al. 2008).
[c] The total B-band luminosity of the MW is quite uncertain; we adopt $(2.0 \pm 0.6) \times 10^{10}\, L_{\odot}^{B}$ (van der Kruit 1987).

than our detection limit, the simulated transient would have been detected. The fraction of detected simulated transients, multiplied by the time window each galaxy was observed, gives the control time. The uncertainty on the detection limits (right panel of Figure 2) are reported as systematic errors, while the three extinction distributions used (low, similar to SNe Ia and high extinction) are reported separately.

During the 13 months of the search, the average number of observed frames per galaxy was 64, while the average control time per galaxy was 80 days. This means that any fast-evolving transients like AT 2017gfo/DLT17ck would likely not be detected a second time if the survey cadence was 2 days or larger. Our strategy of triggering a confirmation image for each new target within a few hours of the first detection well fits the need for these fast transients. Excluding AT 2017gfo/DLT17ck, which was discovered only thanks to the LIGO/Virgo trigger, no other transient with a similar fast evolution was detected. We infer a limit to the rate of kilonovae of $<0.47^{+0.04}_{-0.03}$ SNuB[9](low extinction), $<0.50^{+0.05}_{-0.04}$ SNuB (SNe Ia extinction), and $<0.55^{+0.07}_{-0.05}$ SNuB (high extinction), where the rate has been normalized to the galaxy integrated luminosity. This translates to a limit in our Galaxy of $<0.94^{+0.38}_{-0.37}$ (low extinction), $<1.00^{+0.43}_{-0.36}$ (SN Ia extinction), and $<1.10^{+0.51}_{-0.40}$ (high extinction) per 100 years. These limits and the systematic error are reported in Table 2. As a cross check, we have also computed from DLT40 the SN rates for SNe Ia, Ibc, and II that will be reported in a dedicated paper (S. Yang et al. 2017, in

[9] SNuB = 1SN per 100 years per $10^{10}\, L_{B_{\odot}}$.

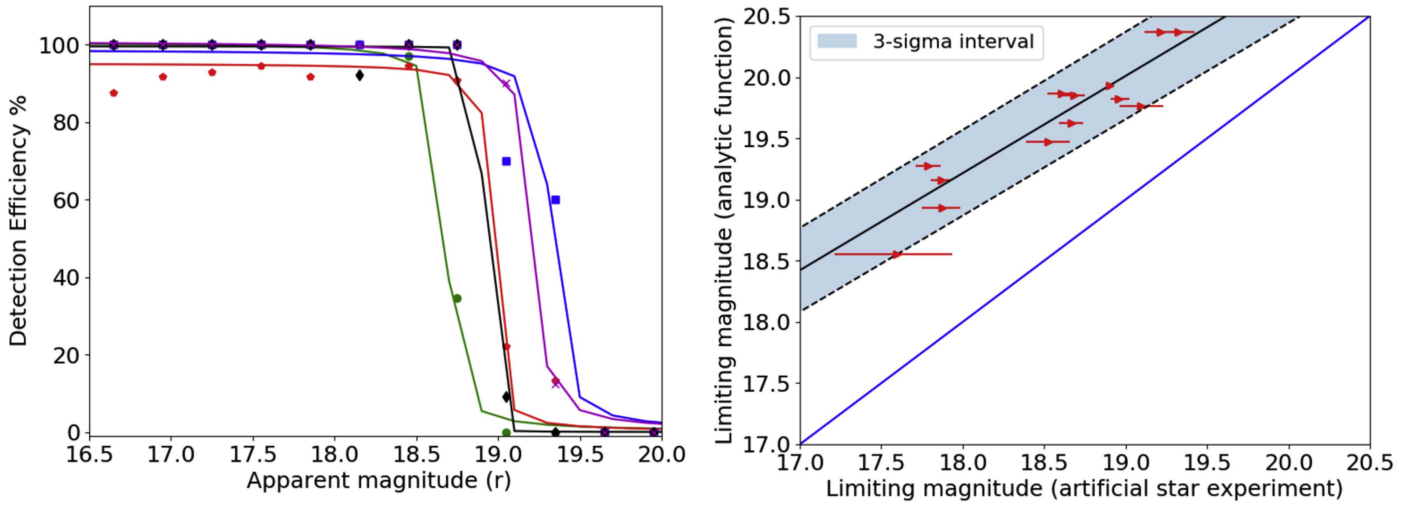

Figure 2. Left panel: transient detection efficiency as a function of apparent magnitude for five DLT40 fields. The lines are the best fit to the curve. The limiting magnitude is chosen at 50% efficiency. Right panel: we compare the limiting magnitude computed for each image using its zeropoint and an analytical function with the limiting magnitude computed with artificial star experiments on difference images. This linear relation has been used to scale the limiting magnitude computed for each frame (given its zeropoint) to a more realistic limiting magnitude estimate for SN and/or kilonova detection.

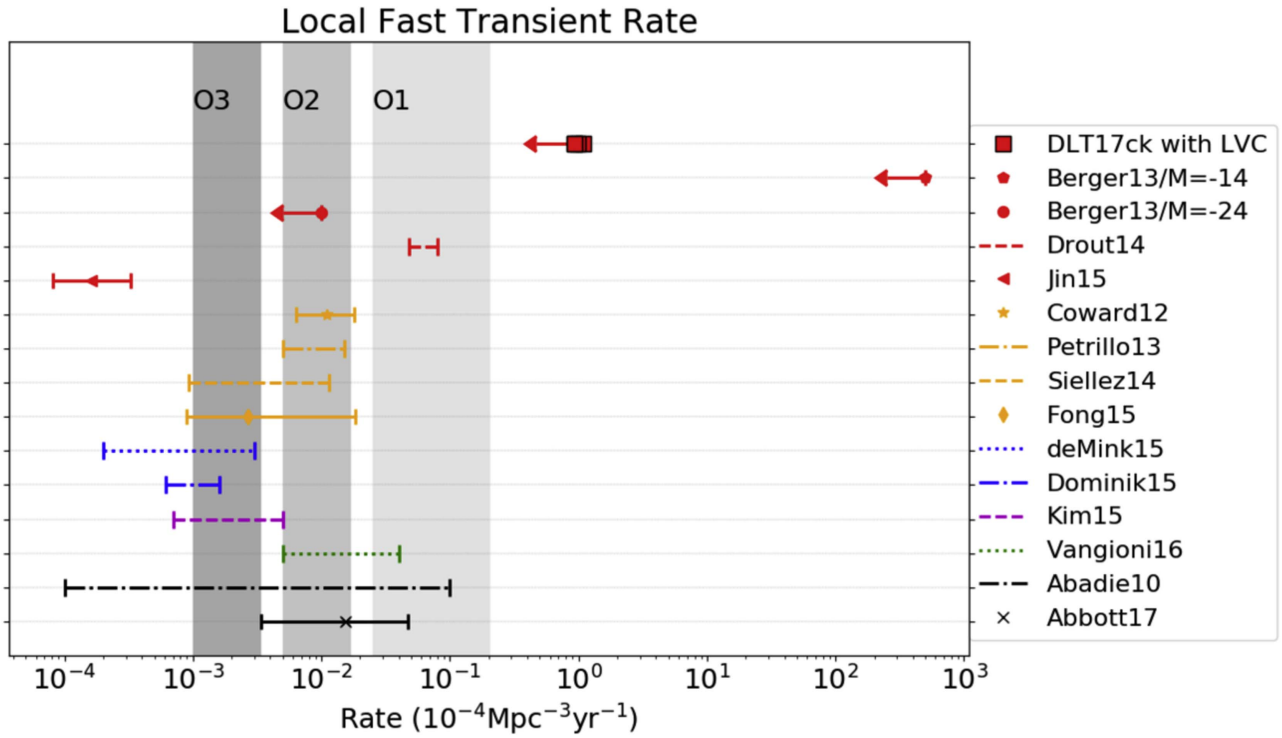

Figure 3. DLT40 limit on the kilonova rate (all three reddening scenarios) compared with the rates of sGRBs (orange symbols; Coward et al. 2012; Petrillo et al. 2013; Siellez et al. 2014; Fong et al. 2015; Scolnic et al. 2017), the rates of BNS merger from stellar evolution (blue lines; de Mink & Belczynski 2015; Dominik et al. 2015), cosmic nucleosynthesis (green line; Vangioni et al. 2016), galactic pulsar population (magenta line; Kim et al. 2015), gravitational waves (black lines; Abadie et al. 2010; Abbott et al. 2017a), and fast optical transients (red symbols; Berger et al. 2013; Drout et al. 2014; Jin et al. 2015).

preparation). We stress that our SN rate estimates are consistent with previous measurements (Cappellaro et al. 1993, 1997; Leaman et al. 2011), despite the poor statistics from a few simplifications in the calculation of the control time.

4. Summary and Future Prospects

In this Letter, we have used the observed light curve of a kilonova to constrain the rate of BNS mergers to less than $0.47^{+0.04}_{-0.03}$ SNuB (low extinction), $0.50^{+0.05}_{-0.04}$ SNuB (SNe Ia extinction), and $0.55^{+0.07}_{-0.05}$ SNuB (high extinction). Since some published measurements of the BNS coalescence rates are expressed in units of comoving volume, we convert SNu rates to volumetric rates similarly to Botticella et al. (2012), that is, multiplying the SNuB rate by the galaxy B-band luminosity density reported in Kopparapu et al. (2008), $(1.98 \pm 0.16) \times 10^{-2} \times 10^{10}\, L_{\odot}^{B}$ Mpc^3. The kilonova volumetric rate upper limit is $0.93^{+0.16}_{-0.18}\ 10^{-4}$ Mpc^{-3} yr^{-1}, $0.99^{+0.19}_{-0.15}\ 10^{-4}$ Mpc^{-3} yr^{-1}, or $1.09^{+0.28}_{-0.18}\ 10^{-4}$ Mpc^{-3} yr^{-1} (depending on the extinction law used) and is compared with previous measurements in Figure 3. Our rate is one order of magnitude higher than the BNS merger

rate limit obtained by LIGO/Virgo during the observing run O1 (Abadie et al. 2010) and two orders of magnitude higher than the optimistic rates of short GRBs (Coward et al. 2012; Petrillo et al. 2013; Siellez et al. 2014).

We can also investigate how long it would on average take for our search to discover (independently from LIGO/Virgo) a kilonova. During the LIGO O2 run (∼1 year), 117 days of simultaneous LIGO-detector observing time has been used to discover one BNS coalescence (Abbott et al. 2017a), which means there are $1/(117/365) = 3.12$ BNS sources in the LIGO searching volume, while our control time for kilonovae in the same period (monitoring galaxies within 40 Mpc) is 0.22 year (on average 80 days per year per galaxy). Comparing the total luminosity of the DLT40 galaxy sample and the total luminosity of the GWGC catalog, within 40 Mpc, gives 60% of the GWGC catalog sample monitored by the DLT40 survey. In order to independently discover a kilonova we would need to run the DLT40 for 3.12/(control time * completeness) × the volume ratio of the two surveys aLIGO/aVirgo and DLT40. During the O2 run, aLIGO/aVirgo were sensitive up to a volume of 78.5 Mpc (Abbott et al. 2016b) and taking into account the different volumes of the two surveys $(78.5/40)^3$, we would need to run DLT40 for ∼18.4 years in order to independently discover a kilonova. This explains why historical optical searches (like the Lick SN search; Leaman et al. 2011) never detected a kilonova.

Given that it is quite unlikely to independently discover a kilonova with a search like DLT40, we may at least understand what a DLT40-like search may be able to do during the O3 aLIGO/aVirgo run. During O3, LIGO will be able to detect BNS coalescences out to 150 Mpc, while Virgo should be sensitive out to 65–85 Mpc (Abbott et al. 2016a). If all kilonovae were as bright as DLT17ck, with the current DLT40 observing strategy, we could detect kilonovae within a distance of 70 Mpc. In order to cover the full Virgo volume (85 Mpc), we would need to go ∼0.4 mag deeper (to a limiting magnitude of ∼19.4 mag), hence increasing the exposure time by a factor of 2.2 (100 s per exposure, instead of the current 45 s). As DLT40 currently observes 400–600 galaxies per night with 45 s exposures, increasing the exposure time to 100 s would still allow us to observe ∼230 galaxies during a single night. Randomly selecting galaxies within 85 Mpc from the GLADE[10] catalog in typical aLIGO/aVirgo regions (30 deg^2), the average number of galaxies is ∼230—almost exactly the same number of galaxies observable by DLT40 each night with an exposure time of 100 s. Here, we neglect that the GLADE catalog is only ∼85%–90% complete in the integrated luminosity up to 85 Mpc (GLADE catalog).

Therefore, within 85 Mpc, small telescopes can still play a useful role (unless DLT17ck turns out to be a particularly bright kilonova), but the incompleteness of the available catalogs, especially for faint galaxies, may suggest that a wide-FoV strategy to directly tile the full aLIGO/aVirgo localization region may be preferred to avoid possible biases in sampling of the stellar population. In this respect, the association of GRBs (Savaglio et al. 2009) and super luminous supernovae (SLSN; Perley et al. 2016) with dwarf galaxies is a lesson learned.

Research by D.J.S. and L.T. is supported by NSF grants AST-1412504 and AST-1517649. The structure of the DLT40 web pages were developed at the Aspen Center for Physics, which is supported by National Science Foundation grant PHY-1066293 A.C. acknowledges support from the NSF award #1455090 "CAREER: Radio and gravitational-wave emission from the largest explosions since the Big Bang." The work of S.Y. was supported by the China Scholarship Council (No. 201506040044).

[10] http://aquarius.elte.hu/glade/

ORCID iDs

Sheng Yang https://orcid.org/0000-0002-2898-6532
Stefano Valenti https://orcid.org/0000-0001-8818-0795
Enrico Cappellaro https://orcid.org/0000-0001-5008-8619
Leonardo Tartaglia https://orcid.org/0000-0003-3433-1492
Alessandra Corsi https://orcid.org/0000-0001-8104-3536
Daniel E. Reichart https://orcid.org/0000-0002-5060-3673

References

Abadie, J., Abbott, B. P., Abbott, R., et al. 2010, CQGra, 27, 173001
Abbott, B. P., Abbott, R., Abbott, T. D., et al. 2016a, LRR, 19, 1
Abbott, B. P., Abbott, R., Abbott, T. D., et al. 2016b, ApJL, 832, L21
Abbott, B. P., Abbott, R., Abbott, T. D., et al. 2017a, PhRvL, 119, 161101
Abbott, B. P., Abbott, R., Abbott, T. D., et al. 2017b, ApJL, 1, L21
Becker, A. 2015, HOTPANTS: High Order Transform of PSF ANd Template Subtraction, Astrophysics Source Code Library, ascl:1504.004
Berger, E., Leibler, C. N., Chornock, R., et al. 2013, ApJ, 779, 18
Botticella, M. T., Smartt, S. J., Kennicutt, R. C., et al. 2012, A&A, 537, A132
Brown, T. M., Baliber, N., Bianco, F. B., et al. 2013, PASP, 125, 1031
Cappellaro, E., Turatto, M., Benetti, S., et al. 1993, A&A, 268, 472
Cappellaro, E., Turatto, M., Tsvetkov, D. Y., et al. 1997, A&A, 322, 431
Coward, D. M., Howell, E. J., Piran, T., et al. 2012, MNRAS, 425, 2668
de Mink, S. E., & Belczynski, K. 2015, ApJ, 814, 58
Doctor, Z., Kessler, R., Chen, H. Y., et al. 2017, ApJ, 837, 57
Dominik, M., Berti, E., O'Shaughnessy, R., et al. 2015, ApJ, 806, 263
Drout, M. R., Chornock, R., Soderberg, A. M., et al. 2014, ApJ, 794, 23
Fong, W., Berger, E., Chornock, R., et al. 2013, ApJ, 769, 56
Fong, W., Berger, E., Margutti, R., & Zauderer, B. A. 2015, ApJ, 815, 102
Gehrels, N. 1986, ApJ, 303, 336
Hulse, R. A., & Taylor, J. H. 1975, ApJL, 195, L51
Jin, Z.-P., Hotokezaka, K., Li, X., et al. 2016, NatCo, 7, 12898
Jin, Z.-P., Li, X., Cano, Z., et al. 2015, ApJL, 811, L22
Kalogera, V., Kim, C., Lorimer, D. R., et al. 2004, ApJL, 601, L179
Kasen, D., Badnell, N. R., & Barnes, J. 2013, ApJ, 774, 25
Kasliwal, M. M., Cenko, S. B., Kulkarni, S. R., et al. 2011, ApJ, 735, 94
Kessler, R., Becker, A. C., Cinabro, D., et al. 2009, ApJS, 185, 32
Kim, C., Perera, B. B. P., & McLaughlin, M. A. 2015, MNRAS, 448, 928
Kopparapu, R. K., Hanna, C., Kalogera, V., et al. 2008, ApJ, 675, 1459
Lattimer, J. M. 2012, ARNPS, 62, 485
Leaman, J., Li, W., Chornock, R., & Filippenko, A. V. 2011, MNRAS, 412, 1419
LIGO Scientific Collaboration & Virgo Collaboration 2017a, GCN, 21509
LIGO Scientific Collaboration & Virgo Collaboration 2017b, GCN, 21527
Metzger, B. D., Martínez-Pinedo, G., Darbha, S., et al. 2010, MNRAS, 406, 2650
Perley, D. A., Quimby, R. M., Yan, L., et al. 2016, ApJ, 830, 13
Petrillo, C. E., Dietz, A., & Cavaglià, M. 2013, ApJ, 767, 140
Piran, T., Nakar, E., & Rosswog, S. 2013, MNRAS, 430, 2121
Reichart, D., Nysewander, M., Moran, J., et al. 2005, NCimC, 28, 767
Savaglio, S., Glazebrook, K., & Le Borgne, D. 2009, ApJ, 691, 182
Scolnic, D., Kessler, R., & Brout, D. 2017, ApJL, submitted (arXiv:1710.05845)
Siellez, K., Boër, M., & Gendre, B. 2014, MNRAS, 437, 649
Tartaglia, L., Sand, D. J., Valenti, S., et al. 2017, ApJ, submitted (arXiv:1711.03940)
Valenti, S., David, J., Soung, S., et al. 2017, ApJL, 848, 2
van der Kruit, P. C. 1987, A&A, 173, 59
Vangioni, E., Goriely, S., Daigne, F., François, P., & Belczynski, K. 2016, MNRAS, 455, 17
White, D. J., Daw, E. J., & Dhillon, V. S. 2011, CQGra, 28, 085016
Zwicky, F. 1942, ApJ, 96, 28